ORIGINAL ARTICLE

European Archives of Medical Research

DOI: 10.14744/eamr.2026.97097
Eur Arch Med Res 2026;42(3):309-321

Which Ankle Morphological Features are Associated with Anterior Talofibular Ligament Injury? An Ordinal Regression Analysis

Enver Ipek,[1] Yusuf Sulek,[2] Oguzhan Nayman,[2] Yusuf Altuntas,[1] Bahadir Balkanli,[1] Tunca Cingoz,[3] Osman Tugrul Eren[1]

[1]Department of Orthopaedics and Traumatology, University of Health Sciences, Şişli Hamidiye Etfal Training and Research Hospital, Istanbul, Türkiye
[2]Department of Orthopaedics and Traumatology, Esenyurt Necmi Kadıoğlu State Hospital, Istanbul, Türkiye
[3]Department of Orthopaedics and Traumatology, Acıbadem University School of Medicine, Istanbul, Türkiye

ABSTRACT

Objective: The objective of the study was to determine whether distal tibiofibular and talar morphological features are associated with the severity of anterior talofibular ligament (ATFL) injury after acute lateral ankle sprain.

Materials and Methods: This retrospective observational study included 280 adults who underwent magnetic resonance imaging (MRI) for acute lateral ankle sprain between January 2018 and December 2024. ATFL injury was classified according to the four-level Schneck system (grade 0–III); using a grade-stratified design, 70 patients were selected at random within each grade. Eighteen radiographic and MRI-based morphological parameters were assessed by blinded observers. Between-grade comparisons used univariate tests with false discovery rate correction. Independent associations with increasing ATFL injury grade were evaluated using ordinal logistic regression.

Results: Nine of 18 morphological parameters differed significantly across injury grades after false discovery rate correction. In the multivariable ordinal model, a smaller talar radius (odds ratio [OR]=0.761/mm, 95% confidence interval [CI]: 0.696–0.832), greater talar height (OR=1.095/mm, 95% CI: 1.047–1.145), higher distal tibial lateral angle (OR=1.112/degree, 95% CI: 1.036–1.195), longer anterior tubercle (OR=1.183/mm, 95% CI: 1.055–1.327), and greater talar dome–distal fibula distance (OR=1.428/mm, 95% CI: 1.124–1.811) were independently associated with higher injury grades. I-type fibular notch morphology was associated with lower odds of a higher grade than C-type morphology (OR=0.295, 95% CI: 0.154–0.564). The model had a Nagelkerke pseudo-R^2 of 0.286.

Conclusion: Talocrural osseous morphology is independently associated with acute ATFL injury severity. These routinely measurable features may contribute to anatomy-informed risk assessment, but the findings are cross-sectional and hypothesis-generating and should not be interpreted as individual-level predictors.

Keywords: Anatomic variation, ankle injuries, anterior talofibular ligament, magnetic resonance imaging, morphometry

Cite this article as: Ipek E, Sulek Y, Nayman O, Altuntas Y, Balkanli B, Cingoz T, et al. Which Ankle Morphological Features are Associated with Anterior Talofibular Ligament Injury? An Ordinal Regression Analysis. Eur Arch Med Res 2026;42(3):309-321.

Address for correspondence: Enver Ipek. Department of Orthopaedics and Traumatology, University of Health Sciences, Şişli Hamidiye Etfal Training and Research Hospital, Istanbul, Türkiye

E-mail: enveripek88@gmail.com **ORCID ID:** 0000-0001-6205-1207

Submitted: 10.08.2026 **Revised:** 24.08.2026 **Accepted:** 28.08.2026 **Available Online:** 18.09.2026

European Archives of Medical Research – Available online at www.eurarchmedres.org

OPEN ACCESS This work is licensed under a Creative Commons Attribution-NonCommercial 4.0 International License.

INTRODUCTION

Ankle sprains are among the most common musculoskeletal injuries in both athletes and the general population, accounting for approximately 5–20% of all sports-related injuries.[1,2] Most of these injuries involve lateral ankle sprains, typically resulting from a plantarflexion–inversion mechanism. The anterior talofibular ligament (ATFL), the weakest component of the lateral ligament complex, is the most frequently injured ligament and may be affected either in isolation or together with the calcaneofibular ligament (CFL).[3] ATFL injuries often present with acute pain, swelling, and functional impairment; if inadequately treated, they can progress to chronic ankle instability (CAI), recurrent sprains, proprioceptive deficits, and, ultimately, post-traumatic osteoarthritis.[4] Previous studies indicate that approximately 20–40% of patients with CAI continue to experience persistent instability and functional limitations despite appropriate rehabilitation.[5]

Recent studies have suggested that, in addition to ligamentous integrity, joint morphology may also play a decisive role in the predisposition to lateral instability. Variations in the distal tibiofibular joint (DTFJ) – such as a shallow or wide tibial incisura, decreased fibular overlap, or an anteriorly positioned fibula – may negatively affect ankle stability.[6-11] Likewise, talar morphology influences the orientation of the articular contact surfaces and load distribution. Asymmetry between the medial and lateral radii of curvature of the talar dome has been proposed to modulate rotatory stabilization and ligament loading,[12] alterations in the orientation of the talar articular facets have been reported in CAI without demonstrable differences in talar curvature,[13] and the osseous configuration of the subtalar joint has also been implicated.[14] These morphological factors may alter the stretching and rupture mechanisms of the ATFL and, when combined with additional risk factors such as high body mass index (BMI) or repetitive microtrauma, may increase the likelihood of injury. However, studies investigating these associations remain limited and report conflicting results; while some researchers have identified significant relationships between distal tibial incisura depth and chronic instability, others have not confirmed this link.[7,9-11,15] Moreover, most previous studies have relied on single-parameter assessments using MRI or radiography alone, and the direct relationships between morphological characteristics, comorbid factors, and ATFL injury severity have not been adequately explored. Consequently, determining whether ligament injury severity is influenced not only by traumatic mechanisms but also by individual anatomical variations remains an important gap in the current literature, and therefore this study was designed to address this uncertainty.

This study aims to investigate the relationship between distal tibiofibular and talar morphology and MRI-determined ATFL injury status. The research question asks whether specific osseous morphological characteristics differ across the four Schneck grades of ATFL injury, from an intact ligament to complete rupture, and whether any such characteristics are independently associated with injury severity after adjustment for other anatomical and demographic factors. The working hypothesis is that morphological variations of the DTFJ and the talar dome are associated with ATFL injury, without a prespecified direction of effect for individual parameters.

MATERIALS AND METHODS

This retrospective observational imaging study was conducted at a single tertiary orthopedic center between January 2018 and December 2024. The study protocol was approved by the Institutional Review Board of the Clinical Research Ethics Committee of University of Health Sciences, Sisli Hamidiye Etfal Training and Research Hospital (IRB no: 5097, date: September 30, 2025) and performed in accordance with the ethical standards of the 1964 Declaration of Helsinki and its later amendments. All imaging data were anonymized before analysis, and no additional interventions were undertaken for research purposes. All magnetic resonance imaging (MRI) and radiographic examinations were retrieved from the institutional Picture Archiving and Communication System (PACS). MRI scans were obtained using a 1.5-T system with standard ankle protocols, including axial, coronal, and sagittal proton density–fat suppressed (PD-FS) or T2-weighted sequences (slice thickness: 3 mm, matrix: 256×256). Standardized radiographs – anteroposterior mortise views of the ankle at 15–20° internal rotation, lateral ankle views, and dorsoplantar foot views – were acquired within ±4 weeks of MRI evaluation. All radiographs were obtained under weight-bearing conditions in accordance with the standard institutional protocol.

Patients who underwent MRI for acute lateral ankle sprain within the study period were retrospectively reviewed. Individuals aged 18 years or older were eligible. Acute lateral ankle sprain was defined based on a compatible trauma mechanism (inversion/plantarflexion injury), acute onset of lateral ankle pain and swelling within 7 days of trauma, and physical examination findings including localized tenderness over the ATFL and/or CFL, and positive anterior drawer or talar tilt tests. MRI confirmation required imaging findings consistent with an acute lateral ankle sprain, including soft-tissue edema, joint effusion, or signal alteration of the lateral ligament complex. Patients in whom the ATFL was intact on MRI despite a clinically confirmed acute sprain were classified as Schneck grade 0. Inclusion criteria were: (1) Evaluable MRI

findings regarding the integrity or rupture of the ATFL, and (2) availability of a complete standardized radiographic series, including weight-bearing mortise and lateral ankle radiographs and a weight-bearing dorsoplantar foot radiograph, obtained within ±4 weeks of MRI. Height and weight recorded in the hospital information system at the time of the index admission were used to calculate BMI. Exclusion criteria included prior ankle surgery or fracture, high-grade syndesmotic injury or deltoid ligament rupture, osteochondral lesions larger than 10 mm, advanced degenerative or inflammatory arthropathies, and poor-quality or non-standard images. Osteochondral lesions larger than 10 mm were excluded because associated subchondral collapse or contour irregularity of the talar dome would compromise the reliability of the talar radius, talar height, and tibiotalar sector angle measurements. Patients meeting all criteria were included in the final analysis (Fig. 1).

The primary dependent variable was the degree of ATFL injury graded on MRI according to the Schneck et al. classification system: Grade 0, intact ligament; Grade I, preserved continuity with increased signal intensity or stretching; Grade II, partial tear; and Grade III, complete rupture or non-visualization of the ligament.[16] All four grades were analysed as a four-level ordinal outcome variable without collapsing categories. ATFL grading was performed by two orthopedic surgeons who independently reviewed all MRI examinations and assigned the final grade by consensus. These two observers were not involved in the morphological measurements and were blinded to all radiographic parameters, to the clinical findings, and to the measurements performed by the other observer pair.

Sample Size

An a priori power analysis was performed before data collection. As the primary analysis was planned as an ordinal logistic regression with ATFL injury grade as a four-level ordinal outcome, sample size was estimated using the method described by Whitehead for ordered categorical data.[17] Assuming a balanced distribution across the four Schneck grades, a two-sided alpha of 0.05, and 80% power, a total of 279 patients (approximately 70/grade) was required to detect an odds ratio (OR) of 1.35 or greater per one standard deviation increase in a continuous predictor. A target of 70 patients per Schneck grade was therefore set. Sampling was grade-stratified rather than consecutive: all patients undergoing MRI for acute lateral ankle sprain within the study period were screened, assessed for eligibility, and assigned to their Schneck grade. Within each grade, 70 patients were then selected at random from all eligible patients of that grade using the random case selection function of Statistical Package for the Social Sciences (SPSS), and screening for that grade was stopped once the target was reached. This balanced design was adopted for analytical purposes, to maximize statistical efficiency of the ordinal regression model across all four grades; the resulting 25% distribution per grade is therefore a feature of the sampling frame and does not reflect the population prevalence of ATFL injury grades. Of 400 patients identified, 362 were assessed for eligibility, and 280 were included (Fig. 1).

All morphological assessments were performed digitally on PACS using millimetric calibration by two other orthopedic surgeons with at least 10 years of experience in musculoskeletal trauma and sports surgery, who were not involved in ATFL

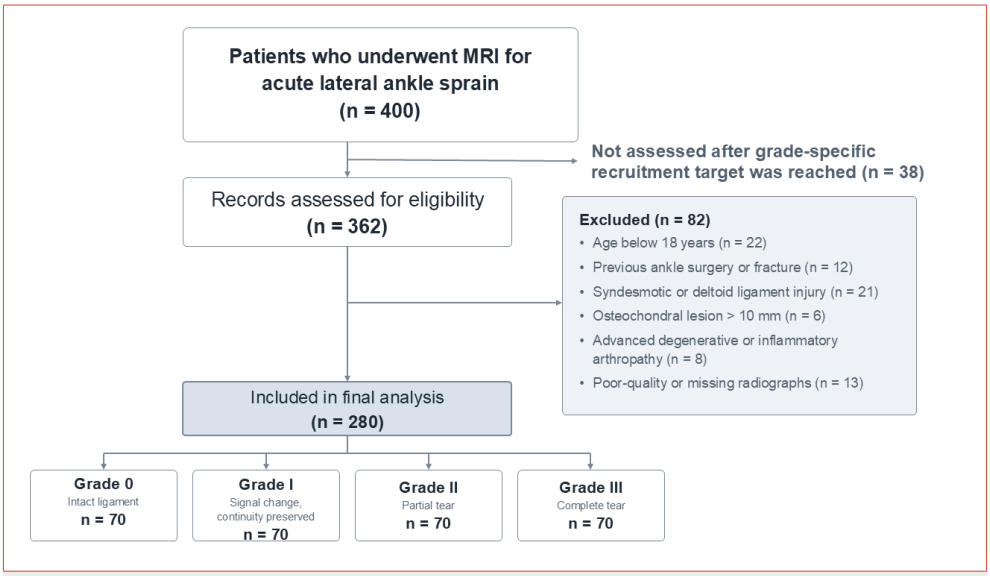


Figure 1. Study flow diagram.

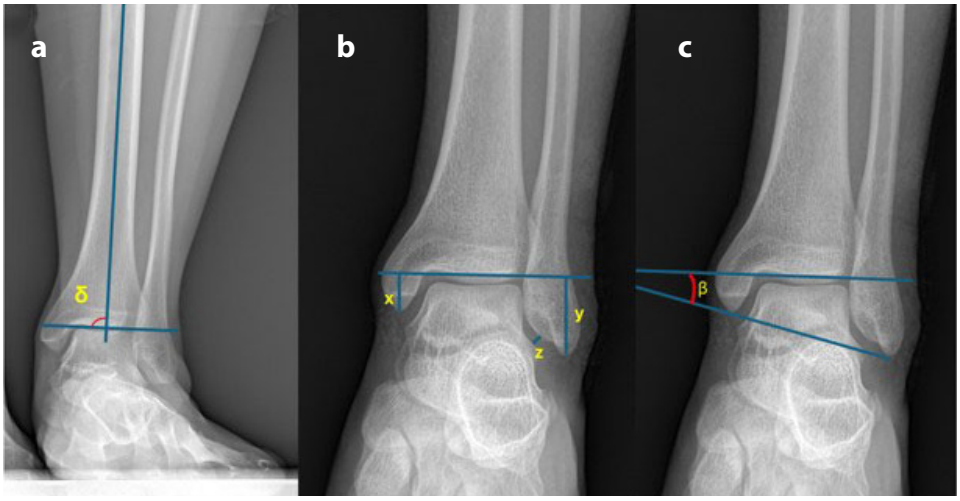


Figure 2. Radiographic measurements on the mortise ankle radiograph. **(a)** Measurement of the distal tibial lateral angle (DTLA), with δ representing the angle between the longitudinal axis of the distal tibial shaft and the tibial plafond line. **(b)** Measurement of medial malleolar length (x, MML), lateral malleolar length (y, LML), and talar dome–distal fibula distance (z, TD-FD). The lateral-to-medial malleolar length ratio (LMMLR) was calculated as y/x. **(c)** Measurement of the talocrural angle (TCA), with β representing the angle between the tibial plafond line and the line connecting the tips of the medial and lateral malleoli.

grading. These observers were blinded to clinical data, to the assigned ATFL injury grade, and to each other's measurements. Radiographic and MRI-based morphological parameters were evaluated.

Morphological Measurements

On radiographs, the distal tibial lateral angle (DTLA, °) was measured on the mortise view as the angle between the longitudinal axis of the distal tibial shaft and the line connecting the most distal articular margins of the tibial plafond (Fig. 2a). Lateral malleolar length (LML) and medial malleolar length (MML) were measured perpendicularly from the tibial plafond line to the distal malleolar tips, and their ratio (lateral-to-MML ratio) was calculated. The talar dome–distal fibula distance (TD-FD) represented the shortest horizontal distance between the lateral border of the talar dome and the inner cortex of the distal fibula (Fig. 2b). The talocrural angle (TCA, °) was measured on the mortise radiograph as the angle between a line along the tibial plafond articular surface and a line connecting the tips of the medial and lateral malleoli, with a reported normal range of 8°–15° using this reference method (Fig. 2c).[18]

The talar convexity angle (TCoA, °) was measured on the lateral radiograph according to the method described by Vuurberg et al. Three points were identified: the posterior tubercle of the talus (P1), the most proximal point of the talar dome (P2), and the deepest point of the transition between the talar body and the talar neck (P3). The angle formed between the lines P1–P2 and P2–P3 was recorded as the TCoA (Fig. 3a).[19] A best-fit circle was fitted to the entire articular contour of the talar dome on the lateral radiograph, extending from the anterior to the posterior articular margin, and the talar radius (r, mm) was recorded as the radius of this circle. The tibiotalar sector angle (α, °) was measured as the angle subtended at the center of this circle by two lines directed towards the anterior and posterior margins of the tibial plafond, representing the proportion of the talar dome covered by the tibial plafond. Talar height (h, mm) was measured on the lateral radiograph as the perpendicular distance from the highest point of the talar dome to the inferior talar cortex (Fig. 3b). The fibulotalar angle (FTA, °) was measured on the lateral radiograph as the angle between the longitudinal axis of the fibula and a tangent to the talar dome (Fig. 3c).

Fibular position (FP, %) was calculated on the lateral radiograph as the ratio of posterior displacement of the distal fibula to the total anterior–posterior tibial depth, multiplied by 100 (Fig. 4a). The talocalcaneal angle (TCalA, °) on dorsoplantar foot radiographs was defined as the angle between the longitudinal axes of the talus and calcaneus (Fig. 4b).

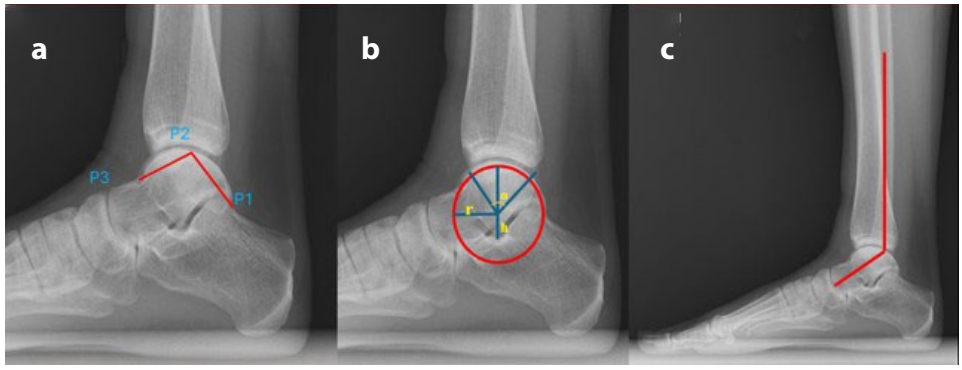


Figure 3. Radiographic measurements of talar morphology on the lateral ankle radiograph. **(a)** Measurement of the talar convexity angle (TCoA). P1 indicates the posterior tubercle of the talus, P2 the most proximal point of the talar dome, and P3 the deepest point of the transition between the talar body and talar neck; the angle P1–P2–P3 represents the TCoA. **(b)** Measurement of the talar radius (r), tibiotalar sector angle (α), and talar height (h) using a best-fit circle of the talar dome. **(c)** Measurement of the fibulotalar angle, defined by the longitudinal axis of the fibula and a tangent to the talar dome.

Fibular notch depth (FND, mm) was measured as the perpendicular distance between the line connecting the tips of the anterior and posterior tibial tubercles and the deepest point of the notch, 10 mm proximal to the tibial plafond, and was analysed as a continuous variable rather than as a classification criterion. The anterior tubercle length (AFL, mm) and posterior tubercle length (PFL, mm) of the fibular notch were measured on axial MRI as described by Mısır et al.,[20]

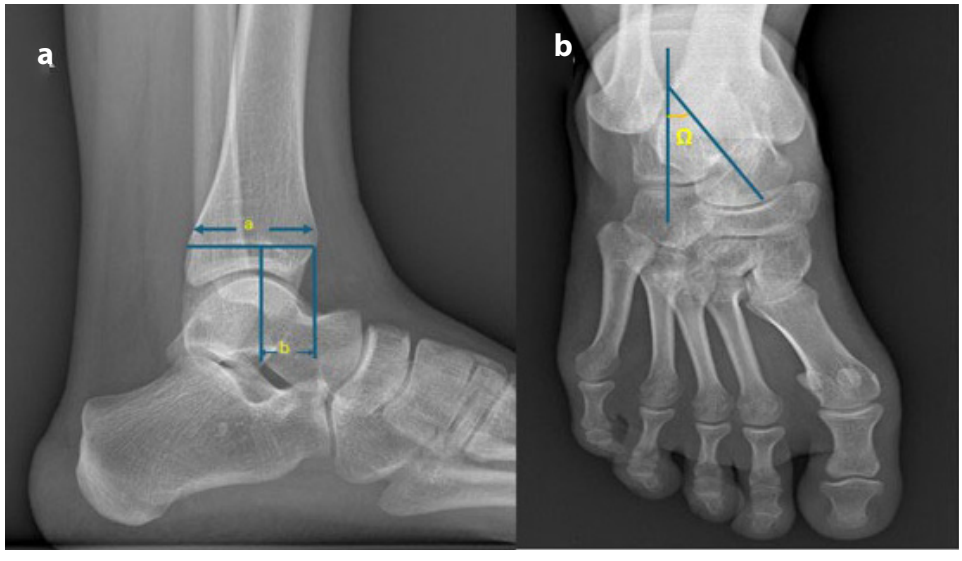


Figure 4. Additional radiographic measurements of ankle and hindfoot morphology. **(a)** Measurement of fibular position (FP). a represents the total anterior–posterior tibial depth and b represents the posterior displacement of the distal fibula; FP was calculated as (b/a) ×100. **(b)** Measurement of the talocalcaneal angle (TCalA) on the dorsoplantar foot radiograph, with Ω representing the angle between the longitudinal axes of the talus and calcaneus.

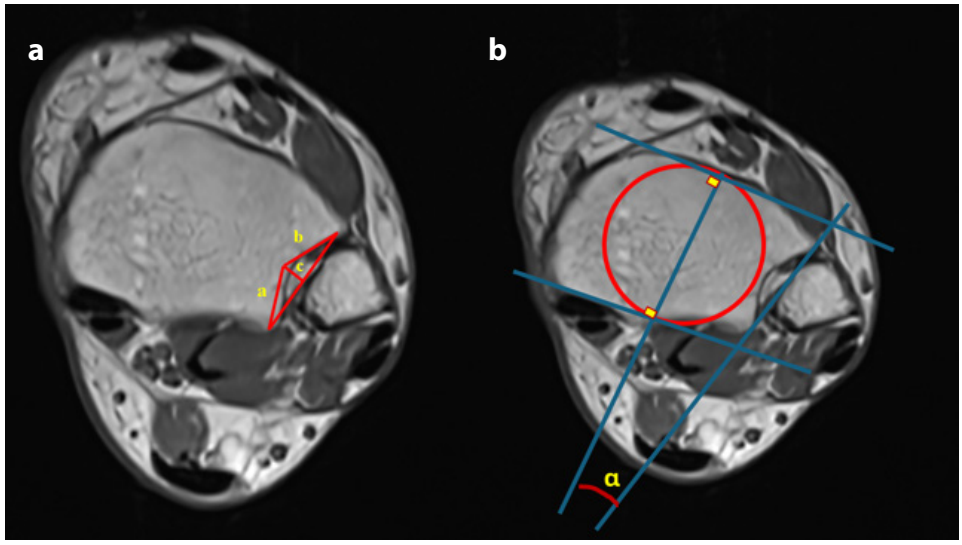


Figure 5. Magnetic resonance imaging-based measurements of fibular notch morphology. **(a)** Measurement of the anterior and posterior tubercle lengths and the anterior–posterior tubercle angle (APFA). a=Represents the posterior tubercle length, b=The anterior tubercle length, and c=The APFA. **(b)** Measurement of fibular notch version, with α=Representing the version angle.

and the angle formed between the anterior and posterior tubercle lines was recorded as the anterior–posterior tubercle angle (APFA, °) (Fig. 5a). The fibular notch version (FNV, °) was measured as the angle between the anterior–posterior axis of the fibular notch and the a line perpendicular to the posterior cortical line of the distal tibia on axial MRI (Fig. 5b).

Fibular notch morphology was classified visually on axial MRI according to the three-type system described by Taser et al.[21] and subsequently applied by Mısır et al.[20] as C-type (concave), I-type (shallow and flat), or r-type (rounded, with a smooth transition between the tubercles) (Fig. 6).

Measurement Reliability

All continuous morphological parameters were measured independently by two observers, and the mean of the two measurements was used for the primary analyses. For reliability

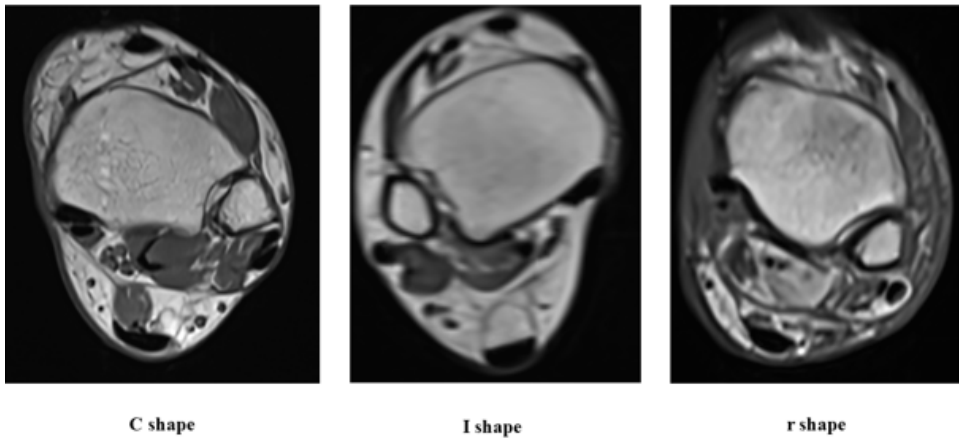


Figure 6. Representative axial magnetic resonance imaging examples of the three fibular notch morphology types: C-type (concave), I-type (shallow and flat), and r-type (rounded, with a smooth transition between the anterior and posterior tibial tubercles).

assessment, a randomly selected subgroup of 30 patients was re-evaluated by the first observer after a 3-week interval. Intraobserver and interobserver reliability for continuous measurements was assessed using intraclass correlation coefficients (ICC; two-way mixed-effects model, absolute agreement, single measures). Agreement for the categorical fibular notch morphology classification was evaluated using Cohen's kappa (κ). Interobserver agreement for the ordinal Schneck grading of ATFL injury was assessed using weighted Cohen's kappa based on the observers' initial independent ratings before consensus.

Potential Sources of Bias

Several potential sources of bias were considered. Selection bias may arise from the grade-stratified sampling design, in which a fixed number of patients were drawn at random from each Schneck grade; this design was adopted to maximize the efficiency of the ordinal model and precludes any inference about the population prevalence of injury grades or the absolute risk associated with a given morphological feature. A further source of selection bias is that only patients referred for MRI after an acute lateral ankle sprain were eligible, so that clinically mild sprains managed without advanced imaging are likely to be under-represented; the single-center tertiary setting may additionally limit generalizability. To minimize measurement bias, ATFL grading and morphological measurements were performed by separate observer pairs; all observers were blinded to the clinical data and to the findings of the other pair; all measurements were performed digitally on millimetrically calibrated PACS images, the mean of two independent measurements was used for each continuous parameter, and intraobserver and interobserver reliability was quantified. Residual confounding cannot be excluded: Age and injury side were included as pre-specified adjustment covariates, but limb dominance, level and type of physical activity, injury mechanism, concomitant CFL involvement, and the interval between trauma and MRI were not available from the retrospective records and could therefore not be modeled.

Statistical Analysis

All statistical analyses were performed using SPSS version 29.0 (IBM Corp., Armonk, NY, USA). Continuous variables were expressed as mean±standard deviation for normally distributed data and as median (25^{th}–75^{th} percentile) for non-normally distributed data, in accordance with the test applied to each variable, and categorical variables as number (percentage). The Shapiro–Wilk test and histogram inspection were used to assess the normality of data distribution. Comparisons across the four ATFL injury grades were conducted using one-way analysis of variance (ANOVA) or the Kruskal–Wallis H test, depending on normality. When significant differences were identified, Bonferroni-corrected post hoc tests were applied for ANOVA and Dunn–Bonferroni post hoc tests for Kruskal–Wallis analyses. Because 18 morphological parameters were compared across injury groups, p-values were adjusted using the Benjamini–Hochberg false discovery rate procedure, and significance was defined as $q<0.05$. Categorical variables were compared using the Chi-square test or Fisher's exact test, as appropriate. To evaluate independent associations between morphological parameters, clinical variables, and the ordinal severity of ATFL injury, an ordinal logistic regression model (proportional odds model) was used. Morphological variables with a p-value below 0.05 in univariate comparisons were considered candidate predictors for the multivariable model. Age and injury side were included as pre-specified adjustment covariates regardless of their univariate p-values. Before fitting the final model, candidate predictors were assessed for multicollinearity, geometric redundancy, and compliance with the proportional odds assumption. Variables with a variance inflation factor (VIF) >5 were excluded because of multicollinearity. The tibiotalar sector angle was excluded because it is geometrically derived from the same best-fit circle as the talar radius. Fibular notch version was excluded because inclusion of this variable resulted in violation of the proportional odds assumption. All remaining candidate predictors and the pre-specified adjustment covariates were entered simultaneously into the final ordinal logistic regression model; no automated stepwise or backward elimination procedure was used. The proportional odds assumption for the final model was verified using the test of parallel lines. For univariate comparisons of morphological parameters, statistical significance was defined as an FDR-adjusted q value below 0.05; for all other analyses, a two-tailed p value below 0.05 was considered significant. No data were missing for any variable.

No artificial intelligence tools or large language models were used in any phase of this study, including study design, data collection, image analysis, statistical analysis, manuscript preparation, or language editing.

RESULTS

Study Population

A total of 280 patients (155 females, 125 males) were included in the final analysis. The median age of the cohort was 44.0 years (25^{th}–75^{th} percentile, 29.0–55.0; range, 18–84), and the median BMI was 27.8 kg/m^2 (25^{th}–75^{th} percentile, 25.0–30.1). The right and left ankles were affected in equal proportions (140 each). By design, each of the four Schneck grades comprised 70 patients (25.0%). Age, BMI, sex, and side did not differ significantly across the four injury grades (Table 1).

Table 1. Demographic characteristics according to ATFL injury grade

Variable	Grade 0 (n=70)	Grade I (n=70)	Grade II (n=70)	Grade III (n=70)	p
Age (years)[a]	41.0 (25.8–54.5)	42.0 (31.8–49.0)	48.0 (32.8–59.3)	48.0 (32.0–54.3)	0.054
BMI (kg/m^2)[a]	28.3 (25.2–30.6)	27.9 (24.3–29.7)	27.8 (25.1–30.5)	27.6 (25.2–30.1)	0.813
Sex (F/M)[b]	37/33	43/27	36/34	39/31	0.645
Side (R/L)[b]	37/33	31/39	29/41	43/27	0.077

Continuous variables are presented as median (25th–75th percentile) and categorical variables as counts. [a]Kruskal–Wallis H test. [b]Chi-square test. BMI: Body mass index; F: Female; M: Male; R: Right; L: Left; ATFL: Anterior talofibular ligament

Fibular Notch Morphology

The distribution of fibular notch morphology differed significantly across injury grades (χ^2=13.50, df=6, p=0.036). The proportion of C-type notches increased progressively from grade 0 to grade III, whereas the proportion of I-type notches declined from 22.9% in grades 0 and I to 7.1% in grade III (Table 2).

Morphological Parameters

Nine of the 18 morphological parameters differed significantly across injury grades after false discovery rate correction (Table 3). Talar radius decreased progressively from grade 0 to grade III (19.54 → 17.22 mm, q<0.001), and anterior tubercle length increased progressively (11.41 → 12.44 mm, q=0.038). Tibiotalar sector angle (q<0.001), talar height (q=0.007), DTLA (q=0.027), and TD-FD (q=0.027) did not change monotonically but had higher median values in grades II and III than in grades 0 and I. Lateral/medial malleolar ratio (q=0.007), fibular notch version (q=0.009), and MML (q=0.027) also differed significantly, without a consistent trend across grades. TCA, fibular notch depth, TCoA, posterior tubercle length, LML, TCalA, fibular position, APFA, and FTA did not differ significantly (q>0.05).

Pairwise Comparisons

Post hoc analysis showed that the main separation occurred between grades without fiber discontinuity (grades 0 and I) and those with a tear (grades II and III). Tibiotalar sector angle did not differ between grades 0 and I (p=1.000) or between grades II and III (p=1.000), but differed significantly across this boundary (grade 0 vs II, p<0.001; grade I vs II, p=0.002). A similar but incomplete pattern was observed for talar height and TD-FD. Apart from fibular notch version, which followed a non-monotonic course across grades, talar radius was the only parameter that also separated grade 0 from grade I (p=0.004), being highest in patients with a fully intact ligament.

Multivariable Analysis

Assessment of multicollinearity identified variance inflation factors above 5 for MML (12.45), lateral/medial malleolar ratio (12.08), and LML (5.44), reflecting the arithmetic dependence between the ratio and its components; these variables were excluded from the multivariable model. All remaining predictors had variance inflation factors below 1.7. Fibular notch version was excluded because the proportional odds assumption was not satisfied when it was included in the model (test of parallel lines, χ^2=36.10, df=18, p=0.007), and the tibiotalar sector angle was excluded because it is geometrically derived from the same best-fit circle as the talar radius.

The ordinal logistic regression model was statistically significant (χ^2=87.29, df=9, p<0.001; Nagelkerke R^2=0.286), and the test of parallel lines was consistent with the proportional odds assumption (χ^2=12.61, df=18, p=0.814). A smaller talar radius (OR=0.761/mm, p<0.001), a greater talar height (OR=1.095/mm, p<0.001), a higher DTLA (OR=1.112 per degree, p=0.004), a longer anterior tubercle (OR=1.183/mm, p=0.004), and a greater TD-FD (OR=1.428/mm, p=0.003) were independently associated with a higher ATFL injury grade. An I-type fibular notch was associated with markedly lower odds of a higher grade than a C-type notch (OR=0.295, p<0.001), whereas the r-type did not differ from the C-type (OR=0.693, p=0.209).

Table 2. Distribution of fibular notch morphology according to ATFL injury grade

Morphology	Grade 0 (n=70)	Grade I (n=70)	Grade II (n=70)	Grade III (n=70)	χ^2	df	p
C-type	37 (52.9)	44 (62.9)	47 (67.1)	53 (75.7)	13.504	6	0.036
I-type	16 (22.9)	16 (22.9)	8 (11.4)	5 (7.1)			
r-type	17 (24.3)	10 (14.3)	15 (21.4)	12 (17.1)			

Values are n (%). Chi-square test. Linear-by-linear association: χ^2=4.180, df=1, p=0.041. ATFL: Anterior talofibular ligament

Table 3. Radiographic and MRI-based morphological parameters according to ATFL injury grade

Parameter	Grade 0 (n=70)	Grade I (n=70)	Grade II (n=70)	Grade III (n=70)	p	q	Significant pairwise comparisons
Talar morphology							
Talar radius (mm)[a]	19.54±2.84	17.99±3.33	17.52±1.85	17.22±2.39	<0.001	<0.001	0 versus I, 0 versus II, 0 versus III
Tibiotalar sector angle (°)[b]	80.34 (71.00–85.30)	79.00 (74.00–86.12)	87.30 (79.72–95.58)	87.10 (82.00–95.33)	<0.001	<0.001	0 versus II, 0 versus III, I versus II, I versus III
Talar height (mm)[b]	31.05 (28.07–35.23)	32.10 (28.25–34.00)	34.40 (30.48–37.58)	33.65 (31.25–37.62)	0.001	0.007	0 versus III, I versus II, I versus III
Talar convexity angle (°)[b]	108.00 (102.00–113.25)	108.00 (103.00–114.25)	105.00 (97.75–115.25)	103.00 (97.75–114.00)	0.129	0.193	—
Fibular notch morphology							
Fibular notch version (°)[b]	32.70 (29.30–37.20)	31.40 (17.50–34.08)	30.85 (26.93–34.55)	32.75 (29.77–37.12)	0.002	0.009	0 versus I, I versus III
Anterior tubercle length (mm)[a]	11.41±2.03	11.77±1.53	12.02±2.21	12.44±2.08	0.019	0.038	0 versus III
Fibular notch depth (mm)[b]	3.75 (3.48–3.90)	3.71 (3.52–3.86)	3.78 (3.56–4.05)	3.75 (3.50–4.09)	0.107	0.174	—
Posterior tubercle length (mm)[b]	11.30 (10.20–12.00)	11.55 (10.07–12.43)	11.70 (10.88–13.53)	11.70 (10.40–14.10)	0.146	0.202	—
AP tubercle angle (°)[b]	138.00 (128.55–149.45)	137.80 (129.38–152.00)	138.55 (130.35–146.43)	135.60 (127.50–142.78)	0.347	0.367	—
Ankle mortise and malleolar morphology							
Lateral/medial malleolar ratio[b]	2.34 (1.84–2.95)	2.12 (1.86–2.53)	2.29 (1.96–2.78)	2.74 (2.07–3.00)	0.002	0.007	I versus III
Distal tibial lateral angle (°)[b]	89.45 (87.28–91.12)	88.90 (88.00–91.20)	90.75 (88.15–92.65)	90.35 (88.45–92.62)	0.012	0.027	—
Medial malleolar length (mm)[b]	10.45 (8.88–13.10)	12.00 (10.20–13.62)	11.55 (9.22–13.03)	10.25 (8.80–11.53)	0.012	0.027	I versus III
Talar dome–distal fibula distance (mm)[b]	3.30 (2.80–4.10)	3.25 (2.67–3.85)	3.70 (3.17–4.28)	3.55 (3.10–4.10)	0.010	0.027	I versus II
Talocrural angle (°)[b]	16.10 (11.32–18.02)	16.00 (12.38–18.30)	14.90 (11.28–17.48)	16.20 (13.88–18.70)	0.067	0.120	—
Lateral malleolar length (mm)[b]	26.20 (23.98–28.93)	25.60 (23.18–28.02)	26.65 (24.02–29.50)	27.05 (24.77–30.00)	0.158	0.203	—
Fibular position (%)[a]	30.35±9.58	28.61±8.36	31.32±11.15	31.47±10.21	0.293	0.330	—
Hindfoot alignment							
Talocalcaneal angle (°)[a]	35.19±6.75	34.27±6.30	36.73±8.01	35.17±6.26	0.202	0.242	—
Fibulotalar angle (°)[b]	131.00 (124.75–143.00)	130.55 (123.00–141.22)	134.00 (119.75–141.25)	134.50 (120.75–145.25)	0.872	0.872	—

Values are presented as mean±SD for variables analyzed using one-way ANOVA and as median (25th–75th percentile) for variables analyzed using the Kruskal–Wallis H test. [a]One-way ANOVA with Bonferroni *post hoc* comparisons; [b]Kruskal–Wallis H test with Dunn–Bonferroni *post hoc* comparisons. q=Benjamini–Hochberg false discovery rate–adjusted p-value across the 18 parameters tested; significance was defined as q<0.05. *Post hoc* pairwise comparisons are reported only for parameters that remained significant after false discovery rate correction (q<0.05). – İndicates no significant pairwise difference. ATFL: Anterior talofibular ligament, MRI: Magnetic resonance imaging.

Table 4. Multivariable ordinal logistic regression model for anterior talofibular ligament injury grade

Variable	OR	95% CI	p
Talar radius (per mm)	0.761	0.696–0.832	<0.001
Talar height (per mm)	1.095	1.047–1.145	<0.001
Distal tibial lateral angle (per degree)	1.112	1.036–1.195	0.004
Anterior tubercle length (per mm)	1.183	1.055–1.327	0.004
Talar dome–distal fibula distance (per mm)	1.428	1.124–1.811	0.003
Fibular notch morphology: I-type (ref. C-type)	0.295	0.154–0.564	<0.001
Fibular notch morphology: r-type (ref. C-type)	0.693	0.392–1.228	0.209
Side: right (ref. left)	1.519	0.973–2.370	0.066
Age (per year)	1.006	0.992–1.020	0.404

Model χ^2=87.29, df=9, p<0.001; Nagelkerke R^2=0.286 (Cox–Snell R^2=0.268; McFadden R^2=0.112). Test of parallel lines: χ^2=12.61, df=18, p=0.814. Threshold estimates: grade 0, 9.688; grade I, 11.094; grade II, 12.459. Reference category for injury side is the left ankle, and for fibular notch morphology, the C-type notch. Odds ratios above 1 indicate higher odds of a more severe injury grade. OR: Odds ratio, CI: Confidence interval

Neither injury side (OR=1.519, 95% confidence interval [CI]: 0.973–2.370, p=0.066) nor age (OR=1.006, p=0.404) was independently associated with injury grade (Table 4).

Reliability

Intraobserver ICC values for continuous morphological measurements ranged from 0.87 to 0.97, and interobserver ICC values ranged from 0.82 to 0.95, indicating good to excellent reliability. Interobserver agreement for fibular notch morphology classification was substantial (κ=0.79). Interobserver agreement for Schneck grading of ATFL injury was also substantial (weighted κ=0.75).

DISCUSSION

The principal finding of this study is that osseous morphology at the level of the talocrural joint is independently associated with the severity of acute ATFL injury. In a balanced cohort of 280 patients distributed evenly across the four Schneck grades, a smaller talar radius, a greater talar height, a higher DTLA, a longer anterior tubercle of the fibular notch, a greater TD-FD, and a C-type rather than an I-type fibular notch were each independently associated with a higher injury grade. The model showed modest overall explanatory performance (Nagelkerke R^2=0.286), suggesting that osseous morphology represents only one component of the multifactorial mechanisms associated with ligament injury severity.

This finding must be placed in a conflicting literature. Frigg et al. reported the opposite direction, with a larger talar radius in patients with CAI (21.2±2.4 mm) than in controls (17.7±1.9 mm), and interpreted a larger radius as producing a flatter dome with reduced tibial restraint.[22] Zendeli et al., in contrast, found a smaller talar radius in patients with recurrent instability after a modified Broström–Gould procedure, and attributed the discrepancy to the fact that the earlier measurements were not normalized to body height, which may have introduced bias because taller patients have both larger talar width and larger radii.[23] Three-dimensional analyses of talar articular geometry have found no difference in curvature between patients with chronic instability and controls.[13] Our values (17.2–19.5 mm) fall within the range reported for controls rather than for the instability group,[22] and our direction of effect is consistent with that of Zendeli et al.[23] Direct numerical comparison with that study nevertheless remains limited, because they normalized the talar dimensions to body height whereas the present measurements are reported in absolute units; radiographic technique, however, was comparable, as both studies used weight-bearing views.

The tibiotalar sector angle showed the reverse relationship, increasing from a median of 80.34° in grade 0 to 87.10° in grade III. Within our data, this is internally coherent: a smaller best-fit circle subtends a larger angle at the same plafond width, so a decreasing radius and an increasing sector angle describe the same geometry. However, both Frigg et al.[22] and Zendeli et al.[23] reported a smaller tibiotalar sector in unstable ankles, the latter with a marked difference (69.8° vs. 79.3°). Our finding therefore contradicts the prevailing interpretation that reduced bony containment predisposes to lateral ligament failure.

Two explanations should be considered. First, the populations differ: previous studies examined chronic instability or recurrent instability after surgery,[22,23] whereas the present cohort comprised acute sprains, and our comparison group consisted of patients who had also sustained an inversion

injury but retained an intact ligament. Second, and more speculatively, greater osseous containment may transfer a larger proportion of the inversion load to the ligamentous restraints rather than allowing it to dissipate through talar rotation within the mortise. This hypothesis is consistent with our data but cannot be tested in a cross-sectional design and requires biomechanical confirmation.

An I-type (shallow) notch was associated with substantially lower odds of a higher injury grade than a C-type notch (OR=0.295). The proportion of I-type notches fell from 22.9% in grades 0 and I to 7.1% in grade III. This is the opposite of what would be predicted from the syndesmotic literature, in which a shallow incisura has been linked to a higher incidence of ligamentous ankle injury, although the corresponding systematic review emphasised that not all studies confirmed this association and that methodology was heterogeneous.[11]

The TD-FD was independently associated with a higher injury grade in the multivariable model (OR=1.428/mm), with wider distances observed in the higher injury grades. This measurement reflects the width of the lateral gutter, that is, the transverse clearance between the talus and the fibula, and a wider gutter is generally interpreted as reduced lateral osseous constraint permitting greater talar tilt during an inversion moment. At first sight this appears to conflict with the sector angle finding described above, in which greater rather than lesser osseous containment accompanied higher injury grades. The two measurements, however, describe different planes: the tibiotalar sector angle quantifies sagittal coverage of the talar dome by the tibial plafond, whereas the TD-FD quantifies transverse clearance at the lateral gutter. A configuration combining extensive sagittal coverage with a wide lateral gutter would constrain sagittal translation while permitting coronal tilt, and would therefore be expected to load the ATFL preferentially. This interpretation is consistent with the present data but was not tested directly and requires biomechanical confirmation.

Fibular notch depth, measured as a continuous variable, did not differ across grades (q=0.174), and notch depth did not distinguish the three morphological types in our cohort. This mirrors the observation of Mısır et al., who defined the same three types partly by a 4 mm depth threshold yet found no difference in measured depth between them.[20] Taken together, these observations suggest that morphological type and quantitative notch depth capture different aspects of incisura anatomy and should not be treated as interchangeable.

Fibular notch version was higher in grade III than in grade I, in the same direction reported by Yaka et al. in patients with ATFL rupture.[24] Our absolute values were approximately twice theirs, which reflects a difference in the reference line used and precludes direct numerical comparison. Notably, the median version angle was lowest in grade II rather than in grade 0, and when it was included in the multivariable model the proportional odds assumption was no longer satisfied (test of parallel lines, p=0.007); it was therefore excluded. This non-monotonic behavior should be interpreted with caution.

Post hoc comparisons revealed a consistent pattern: for the tibiotalar sector angle, and partially for talar height and TD-FD, grades 0 and I did not differ from each other, grades II and III did not differ from each other, but the two pairs differed significantly. The morphological signal therefore separates ankles in which the ligament remained continuous from those in which fibre discontinuity occurred, rather than grading the extent of the tear. Apart from fibular notch version, whose course across grades was non-monotonic, only talar radius separated grade 0 from grade I. This distinction matters for interpretation: our data support an association between osseous morphology and whether the ATFL tears, and provide weaker evidence that morphology determines how extensively it tears.

Given the modest explanatory performance of the model (Nagelkerke R^2=0.286), these parameters should not be used to predict injury severity in an individual patient. Their potential value lies at the level of hypothesis generation rather than clinical application. Talar radius, talar height, and TD-FD are obtainable from routine radiographs without additional acquisitions, and it is conceivable that a patient with recurrent inversion injuries who shows a small talar radius, a greater talar height, and a wide lateral gutter might benefit from a lower threshold for structured proprioceptive rehabilitation or bracing. This possibility is speculative: the present study was cross-sectional, did not assess prospective injury risk, recurrence, treatment response, or functional outcomes, and therefore cannot support any anatomy-based treatment recommendation. Prospective studies with clinical endpoints would be required before such an approach could be considered.

Patients were sampled to obtain balanced groups across Schneck grades; the study sample therefore does not reflect the population prevalence of ATFL injury grades, the reported group proportions should not be interpreted as prevalence estimates, and the design does not permit estimation of absolute injury risk associated with any morphological feature. The findings should accordingly be interpreted as associations between morphological characteristics and ATFL injury grade rather than as individual-level predictions. The study is further limited by its retrospective, single-center design, which may restrict generalizability. Functional and clinical stability assessments were not included; therefore, direct correlation

between morphology and functional outcomes could not be analyzed. Minor variations in radiographic projection or ankle positioning may have influenced some measurements. The TCoA has previously been reported to show only moderate interobserver reliability,[19] which should be considered when interpreting this parameter. The absence of a healthy control group limits differentiation between normal anatomical variations and predisposing risk factors. Mechanism of injury, concomitant CFL involvement, and the interval between trauma and MRI were not recorded, and these factors may influence injury severity independently of osseous morphology. The raw linear measurements were analysed in absolute units and were not normalized for body height or foot size; because larger individuals have proportionally larger tarsal dimensions, part of the observed variation in the talar and malleolar measurements may reflect overall body size rather than a configuration specific to ligament injury. Finally, all measurements were performed on two-dimensional images; three-dimensional evaluation could provide more precise morphometric data.

CONCLUSION

Osseous morphology at the talocrural joint is independently associated with the severity of acute ATFL injury. A smaller talar radius, a greater talar height, a higher DTLA, a longer anterior tubercle of the fibular notch, a greater TD-FD, and a C-type rather than an I-type notch configuration were each independently associated with higher injury grades, and the association was driven mainly by the distinction between ligaments that remained continuous and those that tore. These parameters are obtainable from routine radiographs and MRI and may contribute to anatomy-informed risk assessment; however, given the modest explanatory performance of the multivariable model, they should not be regarded as predictors of individual outcomes.

Disclosures

Ethics Committee Approval: The study protocol was approved by the University of Health Sciences, Sisli Hamidiye Etfal Training and Research Hospital Ethics Committee (No: 5097, Date: 30/09/2025).

Informed Consent: Written informed consent was obtained from all individual participants included in the study.

Conflict of Interest: The authors declare that there is no conflict of interest.

Funding: The authors received no financial support for the research and/or authorship of this article.

Use of AI for Writing Assistance: No artificial intelligence (AI)-assisted technologies, including large language models (LLMs), chatbots, or image generators, were used in the design, conduct, analysis, interpretation, or preparation of this study and manuscript.

Authorship Contributions: Concept – EI, OTE; Design – EI, TC; Supervision – EI, OTE; Fundings – ON, BB; Materials – ON, BB; Data collection &/or processing – YS, ON, YA, BB; Analysis and/or interpretation – YS, TC; Literature search – EI, BB; Writing – EI, YS; Critical review – EI, OTE, ON, TC, YA, BB.

Peer-review: Externally peer-reviewed.

REFERENCES

1. Doherty C, Delahunt E, Caulfield B, Hertel J, Ryan J, Bleakley C. The incidence and prevalence of ankle sprain injury: a systematic review and meta-analysis of prospective epidemiological studies. Sports Med 2014;44:123–40.
2. Roos KG, Kerr ZY, Mauntel TC, Djoko A, Dompier TP, Wikstrom EA. The epidemiology of lateral ligament complex ankle sprains in national collegiate athletic association sports. Am J Sports Med 2017;45:201–9.
3. Hunt KJ, Pereira H, Kelley J, Anderson N, Fuld R, Baldini T, et al. The role of calcaneofibular ligament ınjury in ankle ınstability: ımplications for surgical management. Am J Sports Med 2019;47:431–7.
4. Nakasa T, Ikuta Y, Sumii J, Nekomoto A, Adachi N. Characteristics of chronic ankle instability requiring both anterior talofibular and calcaneofibular ligament repair. J Foot Ankle Surg 2022;61:1028–33.
5. Hiller CE, Kilbreath SL, Refshauge KM. Chronic ankle instability: evolution of the model. J Athl Train 2011;46:133–41.
6. Mandarakas M, Pourkazemi F, Sman A, Burns J, Hiller CE. Systematic review of chronic ankle instability in children. J Foot Ankle Res 2014;7:21.
7. Ataoğlu MB, Tokgöz MA, Köktürk A, Ergişi Y, Hatipoğlu MY, Kanatlı U. Radiologic evaluation of the effect of distal tibiofibular joint anatomy on arthroscopically proven ankle instability. Foot Ankle Int 2020;41:223–8.
8. Uğurlu M, Bozkurt M, Demirkale I, Cömert A, Acar HI, Tekdemir I. Anatomy of the lateral complex of the ankle joint in relation to peroneal tendons, distal fibula and talus: a cadaveric study. Eklem Hastalik Cerrahisi 2010;21:153–8.
9. Huang L, Zhang X, Yang S, Qing J, Wu W, Shi H, et al. Association between the distal tibiofibular syndesmosis morphology classification and ankle osteoarthritis: a retrospective study. J Orthop Surg Res 2023;18:566.
10. Huysse W, Burssens A, Peiffer M, Cornelis B, Stufkens SAS, Kerkhoffs GMMJ, et al. Morphometric analysis of the incisura fibularis in patients with unstable high ankle sprains. Skeletal Radiol 2021;50:1141–50.

11. Wittouck L, Vermeir R, Peiffer M, Huysse W, Pringels L, Martinelli N, et al. Ligamentous ankle injuries in relation to the morphology of the incisura fibularis: A systematic review. J ISAKOS 2025;10:100361.
12. Bonnel F, Toullec E, Mabit C, Tourné Y; Sofcot. Chronic ankle instability: biomechanics and pathomechanics of ligaments injury and associated lesions. Orthop Traumatol Surg Res 2010;96:424–32.
13. Kleipool RP, Stufkens SAS, Dahmen J, Vuurberg G, Streekstra GJ, Dobbe JGG, et al. Difference in orientation of the talar articular facets between healthy ankle joints and ankle joints with chronic instability. J Orthop Res 2022;40:695–702.
14. Zhang L, Sun X, Jiang L, Zhou X, Shi H, Yang Y, et al. The morphology of osseous structure in subtalar joint with chronic ankle instability. Foot Ankle Surg 2024;30:74–8.
15. Yüce A, Erkurt N, Yerli M, Saygılı MS, Özkan CB. Morphology of fibular incisura is a deciding factor between posterior malleolus avulsion fracture or syndesmotic ligament injury in ankle fractures. J Foot Ankle Surg 2024;63:18–21.
16. Schneck CD, Mesgarzadeh M, Bonakdarpour A. MR imaging of the most commonly injured ankle ligaments. Part II. Ligament injuries. Radiology 1992;184:507–12.
17. Whitehead J. Sample size calculations for ordered categorical data. Stat Med 1993;12:2257–71.
18. Crone AM, Omar IM, Bronson AM, Mutawakkil MY, Selley RS, Weaver JS, et al. Guide to lower extremity radiologic measurements: part 3 ankle and foot. Skeletal Radiol 2026;55:1487–1511. doi: 10.1007/s00256-026-05188-1.
19. Vuurberg G, Tümer N, Sierevelt I, Dobbe JGG, Hemke R, Wiegerinck JJ, et al. Translation of 3D anatomy to 2D radiographic angle measurements in the ankle joint: validity and Reliability. Foot Ankle Orthop 2022;7:24730114221112945.
20. Misir A, Uzun E, Tokmak TT. Morphology of the incisura fibularis in the Turkish population. Ann Med Res 2021;28:464–70.
21. Taşer F, Toker S, Kilinçoğlu V. Evaluation of morphometric characteristics of the fibular incisura on dry bones. Eklem Hastalik Cerrahisi 2009;20:52–8.
22. Frigg A, Magerkurth O, Valderrabano V, Ledermann HP, Hintermann B. The effect of osseous ankle configuration on chronic ankle instability. Br J Sports Med 2007;41:420–4.
23. Zendeli F, Pflüger P, Viehöfer AF, Hodel S, Wirth SH, Farshad M, et al. A smaller tibiotalar sector is a risk factor for recurrent anterolateral ankle instability after a modified broström-gould procedure. Foot Ankle Int 2024;45:338–47.
24. Yaka H, Özer M, Türkmen F, Demirel A, Kanatli U. The relationship between fibular notch anatomy and ATFL rupture. J Foot Ankle Surg 2023;62:666–70.